Image Analysis Techniques for the Automated Evaluation of Subaxial Subluxation in Cervical Spine X-ray Images

R. Joe Stanley,
Santhosh Seetharaman
*Department of
Electrical and
Computer Engineering,
University of Missouri-
Rolla, Rolla, MO*
stanleyr@umr.edu

L. Rodney Long,
Sameer Antani,
George Thoma,
*Communications
Engineering Branch,
National Library of
Medicine, Bethesda,
MD*
*rlong@mail.nih.gov,
santani@mail.nih.gov,
thoma@nlm.nih.gov*

Edward Downey
*Palmaris Imaging,
Chesterfield, MO*
downeye@usa.net

Abstract

Rheumatoid arthritis is a chronic inflammatory disease affecting synovial joints of the body, especially the hands and feet, spine, knees and hips. For many patients, the cervical spine is associated with rheumatoid arthritis. Subluxation is the abnormal movement of one of the bones that comprise a joint. In this research, image analysis techniques have been investigated for the recognition of cervical spine x-ray images with one or more instances of subaxial subluxation. Receiver operating characteristic curve results are presented, showing potential for subaxial subluxation discrimination on an image-by-image basis.

1. Introduction

Rheumatoid arthritis is a chronic inflammatory disease affecting synovial joints of the body, especially the hands and feet, spine, knees and hips. The cervical spine has been reported to be associated with patients with rheumatoid arthritis [1-6]. The symptom of spinal cord injury depends on the injury location and the injury severity. Subluxation is the abnormal movement of one of the bones that comprise a joint. In the case of the cervical spine, it can be defined as a partial dislocation of one of the vertebrae.

The subluxation in the cervical spine region can be broadly divided into five different categories, including: 1) anterior atlantoaxial subluxation (aAAS), 2) posterior AAS, 3) lateral AAS, 4) atlantoaxial impaction or vertical AAS, and 5) subaxial Subluxation (SAS). The first four categories are called atlantoaxial subluxation [4-8] because the subluxation (partial dislocation) is seen in the atlantoaxial region. Subaxial subluxation (SAS) [2,5,6] can be diagnosed if the posterior margins of the contiguous vertebral bodies are found to be malaligned for noticeable distances on lateral views of the neck. This type of subluxation can be found at any vertebra, unlike the others, which are only concentrated around C1-C2 region. Figure 1 shows an example of subaxial subluxation for C4-C5, obtained from the Online Digital Atlas Version 2.0 developed by the Communications Engineering Branch of the National Library of Medicine (NLM) [9].

The Lister Hill National Center for Biomedical Communications, an R&D division of NLM has built a Web-based Medical Information Retrieval System (WebMIRS) to permit Internet access to databases of x-ray images and associated text data from the National Health and Nutrition Examination Surveys (NHANES) [10]. Part of the initiative to develop WebMIRS is to determine the feasibility of computer-assisted techniques for the analysis of cervical spine x-ray images. Radiographs of the spine provide a practical approach for detecting and assessing vertebral abnormalities. In this research, image analysis techniques were explored to identify x-ray images containing one or more cases of subaxial subluxation.

Figure 1. Subaxial subluxation example for C4-C5, delimited with the white arrow. This example was obtained from the Online Digital Atlas Version 2.0 [9].

The image analysis techniques investigated individual vertebra posterior side area-based features computed between the spine curve representation through the centroids of the cervical spine vertebrae within the image and the curve representation shifted a constant value to the posterior side of the vertebra column. The purpose for computing the area features is to determine the relative shift of the individual vertebra within the spine column that may be characteristic of subaxial subluxation. The technique uses the spatial location of the each vertebra in the spinal column and the variation in its position as a means to detect the presence of subluxation. Using the vertebrae centroids within the x-ray image, a second order, least squares spinal column curve approximation is determined to quantify the degree to which the vertebrae areas within the image are positioned on their posterior sides. The degree of non-conformity to the vertebra centroid spinal column approximation curve of each vertebra were calculated both with respect to the total vertebra area and the posterior vertebral area using pair wise vertebra difference features for C3-C4, C4-C5, and C5-C6. A multi-layer perceptron (MLP) approach was used to identify cervical spine x-ray images containing one or more subaxial subluxation cases. The approach for subaxial subluxation discrimination is presented as follows: 1) pairwise vertebrae feature extraction algorithm, 2) experiments performed, 3) experimental results and discussion, and 4) conclusions.

2. Pairwise vertebrae extraction algorithm

In order to characterize subaxial subluxation in pairwise vertebrae, a difference feature-based approach was examined. Features for individual vertebra were computed and differenced with adjacent vertebra. Difference features were computed for cervical vertebrae C3-C4, C4-C5, and C5-C6 within each x-ray image. Aggregating the features from the pairwise vertebrae cases, subluxation discrimination was performed on an image-by-image basis.

A general description of the algorithm followed to extract cervical, posterior side-based features is given below. Manually drawn vertebrae borders were used for feature calculations.

IEEE
COMPUTER
SOCIETY

The initial step was to compute the centroid of each vertebra within the x-ray image. A second order, least squares curve was fitted through all the centroid points. Note that spine curve approximation included C3-C7 when C7 was clearly discernible in the x-ray image and C3-C6 when C7 was not clearly discernible in the x-ray image. This curve approximates the curvature of the spinal column. Figure 3 shows an image example with the spine curve fitted through the vertebrae centroids, including C3-C7. Figure 2 (a) presents the original cropped grayscale image, and Figure 2 (b) gives the vertebrae borders with the spine curve displayed through the vertebrae centroids.

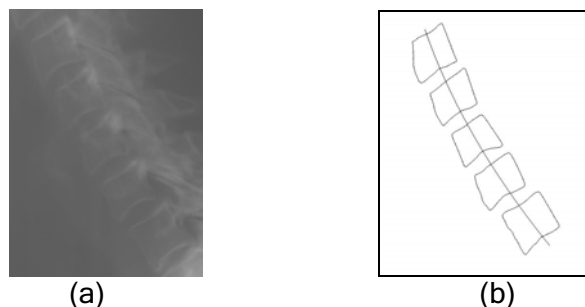(a)   (b)

Figure 2. Image example of spine curve approximation through vertebrae centroids. (a) Original cropped grayscale image. (b) Individual vertebrae boundaries with spine curve approximation through centroids.

From the spinal curve approximation, a normal linear segment was determined for each vertebra and was extended in the posterior direction to intersect the vertebra boundary. The width of the particular vertebra is the Euclidean distance between centroid and vertebra boundary position where the normal linear extension intersects. The average width overall vertebrae was computed. A set of second-order curves were drawn so as the overlap the posterior sides of the vertebrae, shifting the spine curve incrementally from the original centroids position to the average width on the posterior side of the vertebrae. The resulting strip or band represents the whole spinal column. Any vertebra that does not lie within the given band is likely to be subluxed. The amount of area that was protruding out of the band or the amount of area that was missing under the band, i.e. the amount of the non-overlapping area was calculated. Figure 3 gives an image example of the normal segments to the spine curve for the image in Figure 2 (b). Note that the example shows the normal segment going through the anterior and posterior sides. Only the posterior side (right side for the figures) was used for feature calculations. Figure 4 presents the corresponding filled posterior side region associated with the shifted spine curve approximation by the average width of the vertebrae within the image for the image in Figure 2 (b).

Two features were computed for each vertebra based on the strip region between the spinal curve through the centroid points and the spinal curve shifted the median width from the centroid position. The first feature for vertebra i (F_{1i}) normalizes the overlap with respect to the whole vertebrae area, yielding $F_{1i} = \dfrac{B_i}{A_i}$, where B_i is the area of vertebra i contained in the strip region and A_i is the total vertebra area. The second feature for vertebra i (F_2) normalizes the overlap with respect to the posterior region, yielding $F_{2i} = \dfrac{C_i}{A_i}$, where C_i is the vertebra's posterior side area.

The above two features were extended for subluxation discrimination on an image-by-image basis. Subluxation discrimination was treated with respect to neighboring vertebrae. The lateral

distance between the first and the last vertebra in a given spinal column can be large in case of normal vertebra, but the lateral distance between the adjacent vertebrae is the main concern in case of subluxation. The features were made to correspond to adjacent vertebra simply by taking the difference between the feature values. The absolute lateral distance values were converted into relative lateral distance values. The six features used for image-based subluxation discrimination included $F_{1ij} = F_{1i}-F_{1j}$ and $F_{2ij} = F_{2i}-F_{2j}$ for pairwise $(i,j) = (3,4),(4,5),(5,6)$.
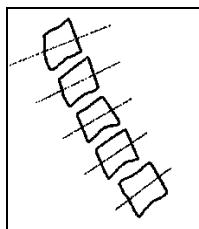

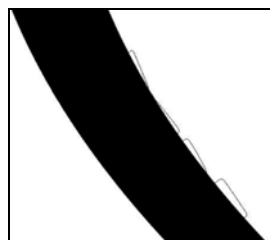Figure 3. Image example of normal segments computed for individual vertebra from the image in Figure 2 (b).

Figure 4. Image example of filled vertebra region using the image shown in Figure 2 (b).

3. Experiments performed

3.1 Data set description

For image analysis technique development, a radiologist labeled subluxed vertebrae cases from the cervical spine x-ray image data set provided by the National Library of Medicine. The Communications Engineering Branch of the National Library of Medicine developed the Online Digital Atlas Version 2.0 in 2000 to provide a digital reference source to assist with the interpretation of cervical and lumbar vertebrae in x-ray images [9]. To guide the radiologist in labeling the subluxed vertebrae cases, the radiologist used the Digital Atlas program for example cases. The tool contains subluxation examples with grades of 0 and 1 for normal and subluxed cases, respectively. Figure 1 shows an example of cervical spine subluxation of grade 1 for levels 4-5 from the Digital Atlas 2.0 application. From Figure 1, the assessment for cervical spine subluxation is based on an adjacent pairwise vertebra assessment. For data truthing, each pair of vertebrae assessed to be subluxed was given a grade of 1, with some extreme cases assigned a grade of 2. Normal pairwise vertebrae cases were given a grade of 0. From the truthed data set, there were a limited number of cases for C6-C7 in compiling the data set. Accordingly, subluxation cases involving C3-C4, C4-C5, and C5-C6 were used for analysis. For feature evaluation, if one or more pairs of vertebrae were given a non-zero grade, the image was labeled as abnormal. If all pairs of vertebrae were assigned a 0 grade, the image was labeled as normal. From the compiled data set, there were 28 images with one or more subluxed vertebrae cases and 80 normal images.

3.2 Description of experiments

The following experiments were performed to evaluate the pairwise difference posterior area-based features for subluxation discrimination on an image-by-image basis. A standard back propagation neural network was investigated. The labeling of the images for discriminating images containing subluxation cases from normal images is to give a 1 for images with one or

more subluxation cases and a 0 for normal images. Due to the limited number of images with subluxation cases, a leave-one-out MLP approach was used for feature evaluation.

The following procedure was used for the leave-one-out approach. First, feature normalized was performed by subtracting the mean of each feature value from the training set and dividing by the standard deviation of each feature value from the training set. Second, the neural network architecture used was 6x6x3x1, meaning 6 feature inputs, 6 nodes in the first hidden layer, 3 nodes in the second hidden layer, and 1 output node. The transfer functions used were log sigmoid for the first and second hidden layers and linear for the output layer. Third, the neural network training procedure was to begin at 5 epochs and to terminate training at 15 epochs or when the training error was less than or equal to 0.09. Fourth, a receiver operating characteristic (ROC) curve was used to evaluate the leave-one-out neural network results. The MLP output was thresholded in 200 unit intervals between the maximum and minimum subluxed case output values. For each threshold, an image was considered to contain one or more subluxed cases if the output value exceeded the threshold. Otherwise, the image was considered normal.

4. Experimental results and discussion

A leave-one-out MLP was used to evaluate the adjacent vertebra posterior area-based difference features for subluxation discrimination on an image-by-image basis. Figure 5 shows the ROC curve results for discriminating between images that contain one or more subluxed vertebrae and normal images. The vertical axis gives the percentage of images with subluxation cases that were correctly recognized. The horizontal axis provides the percentage of normal images that were called subluxed cases (probability of false alarm). The ROC curve results show 96.4% probability of subluxation detection on an image basis with 3.8% false alarms (normal images labeled subluxed images) and 100% probability of subluxation detection with 23.8% false alarms.

In evaluating the experimental results over the cervical x-ray image data set, there were several issues that must be addressed. First, difference features were used to provide an interpretation of subluxation that is similar to the interpretation of subluxation for the Digital Atlas example utilized for truthing the data, where example cases are shown for grades 0 and 1. Second, based on experimentation, individual subluxation case discrimination for pairwise vertebra for the posterior area-based features was low compared to discrimination results on an image basis. Obtaining a larger data set for subluxation cases would improve multi-layer perceptron training for individual case discrimination.

Third, there is difficulty predicting how the actual spinal curve approximation will change beyond the first (C3) and last (C6) centroid points. An image example of the problematic modeling of the spinal column at the end positions is shown in Figure 6. From Figure 6, the spinal curve is distorted in C6. The result is distorted features computed for C6 and the associated difference features with C5. In this case, the normal image was labeled a subluxed case. We attempted to address this by including C7 in the spine curve approximation (when C7 was clearly discernible in the x-ray image) but excluded feature calculations for C6-C7. Fourth, the technique presented utilizes the posterior side of the vertebra for feature calculations for subluxation discrimination. This assumes that there is a negligible effect from posterior osteophytes or other posterior vertebra anomalies that would distort the feature calculations. Fifth, without providing individual subluxation case discrimination information, the experimental technique flags images where a radiologist can identify the subluxed vertebrae cases. Finally, the truthing of the subluxation cases is binary for discrimination purposes. No information is used in this research describing the degree to which vertebrae are subluxed. The image-based approach for subluxation discrimination circumvents the individual labeling of

subluxed vertebrae, enabling the relative comparison of vertebrae within an image to be used in making a subluxation discrimination decision.
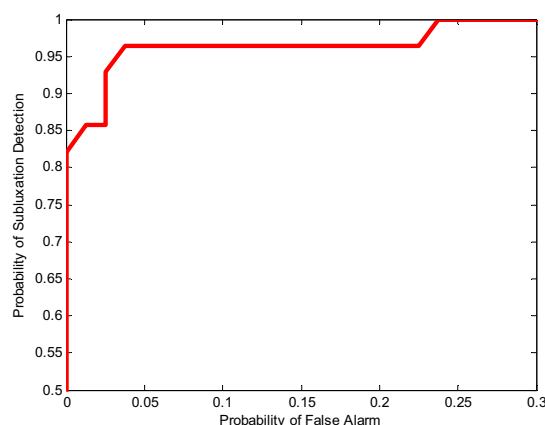

Figure 5. ROC curve results for leave-one-out approach for subluxation discrimination on an image basis for posterior area-based features.
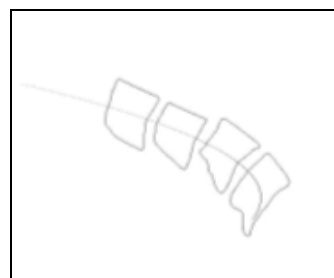

Figure 6. Example of distorted spinal curve from the second order least squares model as seen in C6.

5. Conclusions

In this research, image analysis techniques were introduced to discriminate cervical x-ray images containing one or more cases of subaxial subluxation from normal images. Adjacent vertebra posterior area-based difference features were investigated for discrimination using a leave-one-out multilayer perceptron approach. Experimental ROC curve results showed potential for the features to characterize subluxation for discrimination on an image-by image basis. Future extensions of this research would integrate disc space narrowing features with the minimum distance and posterior area-based features.

6. References

[1] T. K. Kwek, T. W. Lew, and F. L. Thoo, "The role of preoperative cervical spine X-rays in rheumatoid arthritis," Anaesthesia & Intensive Care, 1998, vol. 26, no. 6, pp. 636-41.

[2] D. K. Evans, "Anterior cervical subluxation," Journal of Bone & Joint Surgery, 1976, vol. 58, no. 3, pp. 318-321.

[3] Y. I. Li, Y. K. Zhang, and S. Z. Zhong, "Diagnostic value on signs of subluxation of cervical vertebrae with radiological examination," Journal of Manipulative & Physiological Therapeutic, 1998, vol. 21, no. 9, pp. 617-620.

[4] M. Kauppi and M. H. Neva, "Sensitivity of lateral view cervical spine radiographs taken in the neutral position in atlantoaxial subluxation in rheumatic diseases," Clinical Rheumatology, 1998, vol. 17, no. 6, pp. 511-514.

[5] K. Yoshida, T. Hanyu, and H. E. Takahashi, "Progression of rheumatoid arthritis of the cervical spine: radiographic and clinical evaluation," Journal of Orthopaedic Science, 1999, vol. 4, no. 6, pp. 399-406.

[6] K. Laiho, K. Kaarela, and M. Kauppi, "Cervical spine disorders in patients with rheumatoid arthritis and amyloidosis," Clinical Rheumatology, 2002, vol. 21, no. 3, pp. 227-230.

[7] J. C. Oostveen, A. R. Roozeboom, M. A. van de Laar, J. Heeres, J. A. den Boer, and S. F. Lindeboom, "Functional turbo spin echo magnetic resonance imaging versus tomography for evaluating cervical spine involvement in rheumatoid arthritis," Spine, 1998, vol. 23, no. 11, pp. 1237-1244.

[8] K. Laiho, I. Soini, H. Kautiainen, and M. Kauppi, "Can we rely on magnetic resonance imaging when evaluating unstable atlantoaxial subluxation?" Annals of the Rheumatic Diseases, 2003, vol. 62, pp. 254-256.

[9] L. R. Long, S. R. Pillemer, G. –H. Goh, L. E. Berman, L. Neve, G. R. Thoma, A. Premkumar, Y. Ostchega, R. C. Lawrence, R. D. Altman, N. E. Lane, and W. W. Scott Jr., "A digital atlas for spinal x-rays," In Proc SPIE Medical Imaging 1997: PACS Design and Evaluation, Newport Beach, CA, 1997, vol. 3035, pp. 586-594.

[10] L. R. Long and G. R. Thoma, "Image query and indexing for digital x-rays," In Proc. SPIE Conference on Storage and Retrieval for Image and Video Databases VII, San Jose, CA, 1999, vol. 3656, pp. 12-21.